Proceedings of the 17th World Congress
The International Federation of Automatic Control
Seoul, Korea, July 6-11, 2008

Hopf Bifurcation and Oscillations in Homogeneous Communication Networks

Huibing Yin * **Paul Wang** * **Tansu Alpcan** ** **Prashant G. Mehta** *

* *Coordinated Science Laboratory,*
Department of Mechanical Science and Engineering,
University of Illinois at Urbana-Champaign,
1206 W. Green Street, Urbana, IL 61801.
yin3,paulwang,mehtapg@uiuc.edu
** *Deutsche Telekom Laboratories, Ernst-Reuter-Platz 7, 10587 Germany*
tansu.alpcan@telekom.de

Abstract: In this paper, we investigate stability and bifurcation arising in a communication network model with a large number of homogeneous (symmetric) users and a single bottleneck AQM queue. We carry out bifurcation analysis to study the effect of user delay and strength of feedback. It is shown that for any given delay, there exists a critical amount of feedback (due to AQM) at which the equilibrium loses stability and a limit cycling solution develops via a super-critical Hopf bifurcation. The conclusion is verified both numerically and analytically.

1. INTRODUCTION

Communication networks such as the Internet exhibit a wide variety of complex dynamic behavior. Examples of such complex behavior include dynamic synchronization of the flows passing through the same bottleneck link [Han et al. (2005)], user flow rate oscillations in the presence of delays [Shakkottai et al. (2003)], and chaotic behavior of user flows and queues at the routers[Veres and Boda (2000)].

This paper is concerned with stability, bifurcation and oscillations arising in communication networks vis-a-vis two important factors: 1) network delay and 2) network inter-connection strength. The type of delay considered models the delay $\sqrt{d}$ that user experiences in receiving feedback from the network. The network inter-connection strength is modeled here using coupling strength parameter β, a parameter in the active queue management (AQM) model. The stability and bifurcation results are described in the parameter space (β, d). The motivation for considering these two factors (more than others) is because: 1) of their physical relevance to communication networks, and 2) these issues are universal, albeit in different forms, across networks. As an example, biological networks are often studied using simplified oscillator models where oscillator frequency is a network parameter and inter-connection is determined by coupling strength and the properties of graph Laplacian; cf., Ariaratnam (2002).

Recently, there have been many papers focussing on dynamics, bifurcation, oscillations and chaos in simplified models of communication networks. One of the earliest papers, Veres and Boda (2000) found (using numerical simulations) that TCP exhibits chaotic behavior regardless of the applications, such as HTTP, SMTP, suggesting that there are inherent chaotic behavior imbedded in TCP. This was verified by La et al. (2002) when they found that the chaotic behavior is also independent of the discontinuities in the drop probability of droptail. Firoiu and Borden (2000) showed that the equilibrium queue value depends on its relation with the drop probability, and Shakkottai et al. proved that the oscillatory TCP flows are in fact bounded.

A variety of analytical methods have been applied to study these oscillations. Ranjan and Abed (2002) found period-doubling and border-collision bifurcation using center manifold theorem on an discrete-time normalized TCP-RED model. Li et al. (2004) used normal form theory and center manifold theorem to find a supercritical Hopf Bifurcation. Raina (2005) obtained results on local bifurcation for a nonlinear delay differential equation model of communication with a single discrete delay. Han et al. (2005) study the question of synchronization of two TCP flows by using a weakly coupled oscillator analogy. An approach based on describing functions analysis of synchronization is described in Korkut (2006).

There are three contributions of this paper: One, we provide analytical methods of a homogeneous network with large number of users. Two, the parameter space (β, d) representing the effects of delay and inter-connectivity are not only relevant from practical considerations but also can be used as benchmark for other investigations with more general network topology. In particular, we present numerical and analytical evidence on role of these two factors and characterize stability of equilibrium solutions, as well as nature of bifurcation and resulting non-equilibrium limit cycling solution. Finally, the results of our analysis can serve as design guidelines for choosing the feedback strength as well as investigating other coupling mechanisms that have better stability and bifurcation characteristics.

The remainder of this paper is organized as follows. In Section 2, we present the fluid model with numerical results on kinds of behavior observed. These numerical results are explained with the aid of linear and nonlinear analysis presented in Sections 3 and 4 respectively. Section 5 concludes with a summary of the work and possible avenues for future research.

2. MODEL AND NUMERICS

2.1 Models

We consider a communication network with a single bottleneck link topology with fixed capacity C shared by M users. Instead of conducting a packet level analysis of the network we adopt a network model based on fluid approximations Srikant (2004); Alpcan and Başar (2005). Each user is associated with a unique connection for simplicity and transmits with a nonnegative flow rate x_i over this bottleneck link. For $x_i \in \mathbb{R}^+ \doteq [0,\infty)$, the i^{th} user is assumed to follow a transfer control protocol (TCP)-like additive-increase multiplicative-decrease flow control scheme:

$$\dot{x}_i(t) = \kappa\left[\frac{1}{d} - \beta x_i(t) x_i(t-\sqrt{d}) p(t-\sqrt{d})\right], \qquad (1)$$

where $0 \le p \le 1$ is the observed rate of marking (or depending on the implementation, dropping) of its packets, $\sqrt{d}$ is the delay and β is the coupling parameter.

The packet marking occurs at the link whose dynamics are next described. If the aggregate sending rate of users exceeds the capacity C of the link, then the arriving packets are queued in the buffer q of the link. The non-negative queue size evolves according to the ODE:

$$\dot{q}(t) = \begin{cases} \sum_{i=1}^{M} x_i(t) - C & \text{if } 0 < q < Q_{max}, \\ \min(0, \sum_{i=1}^{M} x_i(t) - C) & \text{if } q = Q_{max}, \\ \max(0, \sum_{i=1}^{M} x_i(t) - C) & \text{if } q = 0, \end{cases} \qquad (2)$$

where we assume a maximum buffer size of $Q_{\max}$ at which the queue saturates and any incoming packet after this point is dropped; cf. Hollot et al. (2002). $p(\cdot)$ in (1) is set by the AQM control and takes the general form

$$p = f(q). \qquad (3)$$

The analytical results and formulas are presented with feedback form $p = f(q)$. The numerical evidence will be provided for a linear feedback of the type used in a RED type AQM scheme. In particular, $p(t)$ is a linear function of q:

$$p(t) = \frac{q(t)}{Q_{\max}}. \qquad (4)$$

Note that the parameter β is used to scale the amount of feedback.

2.2 Numerical Results

In this section, we present the results on the numerical study of equations (1) and (2). The simulations were carried out in MATLAB for parameter values given in Table 1. For details on numerical approximation, time-step, initial conditions, convergence etc., see Wang (2007). Numerically, there are two kinds of asymptotic behavior observed in the (β, d) parameter space: Equilibrium and limit-cycle Oscillations.

Equilibrium solution: For $\beta = 0$, the queue saturates at $Q_{\max}$ and user flow rates increase without bound. For sufficiently small positive values of parameter β, one asymptotically observes an equilibrium solution for user flow rates and queue.

Table 1. Parameter Values

Link Capacity	$C = 1000$
# of users	$M = 10$
Queue bounds	$Q_{min} = 0,\ Q_{max} = 100$
User parameters	$\kappa = 0.01$

This solution is denoted as $z_0 = (x_0, q_0)^T$, where x_0 is a positive vector of size M. The equilibrium solution x_0 is symmetric, i.e., all users have the same flow rate. $x_0 > \frac{C}{M}$ and $q_0 = Q_{max}$ for $d < d^*(\beta)$, and $x_0 = \frac{C}{M}$ and $q_0 < Q_{max}$ for $d > d^*(\beta)$; see Fig. 1(a). In words, for a given coupling strength β, the queue saturates ($q_0 = Q_{\max}$) leading to an inefficient user flow rate ($x_0 > \frac{C}{M}$) for sufficiently small delays.

Oscillations: For a fixed delay d, we have: a) $x_0 > \frac{C}{M}$ and $q_0 = Q_{max}$ for $\beta \le \beta^*(d)$(this corresponds to the inefficient equilibrium regime); b) $x_0 = \frac{C}{M}$ and $q_0 < Q_{max}$ for $\beta^*(d) < \beta < \beta_0(d)$; and c)large amplitude oscillations appear for $\beta \ge \beta_0(d)$.

The above discussion is summarized in a single bifurcation diagram depicted in the (β, d) parameter space in Figure 1(a). The boundaries $\beta^*(d)$ and $\beta_0(d)$ are indicated. In the following, we present analysis of stability, bifurcation, and oscillations in the efficient regime, i.e., for $\beta > \beta^*(d)$. Our choice is largely dictated by the fact that this regime is the most interesting; more complete results including stability analysis for $\beta \le \beta^*(d)$ appear in Wang (2007).

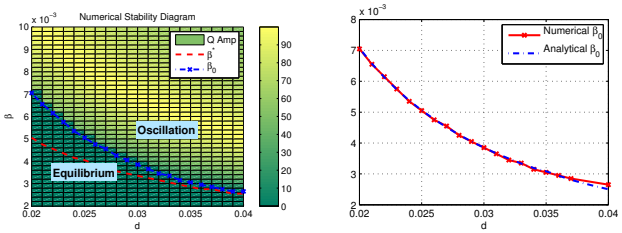

(a) (b)

Fig. 1. (a) Stability diagram calculated numerically with queue amplitude, and (b) Comparison of critical beta between simulation and analytical results

3. LINEAR ANALYSIS

In this section, we obtain formulas for equilibria (Section 3.1) and study its stability via spectral analysis (Section 3.3). The analysis shows the equilibrium looses stability at a critical value of parameter $\beta = \beta_0$. At the crossover point, the eigenvalue is imaginary suggesting the presence of Hopf bifurcation. This is pursued in detail in the following section.

3.1 Equilibrium

The numerical simulations show that the user flow rate is symmetric in both the equilibrium and the oscillatory regimes. To aid the analysis of such solutions, (1)-(2) is replaced by dynamics in the symmetric fixed point space:

$$\dot{x}(t) = \kappa\left[\frac{1}{d} - \beta x(t)x(t-\sqrt{d})p(t-\sqrt{d})\right] \tag{5}$$

$$\dot{q}(t) = \begin{cases} Mx(t) - C & \text{if } 0 < q < Q_{max} \\ \min(Mx(t) - C, 0) & \text{if } q = Q_{max} \\ \max(Mx(t) - C, 0) & \text{if } q = 0. \end{cases} \tag{6}$$

The equilibrium solution, denoted as $z_0 \doteq (x_0, q_0)^T$ is obtained by setting right hand side to 0:

$$z_0 = \begin{cases} \left(\frac{1}{\sqrt{\beta d}}, Q_{max}\right)^T & \text{if } \beta < \beta^*(d) \\ \left(\frac{C}{M}, f^{-1}\left(\frac{\beta^*(d)}{\beta}\right)\right)^T & \text{otherwise} \end{cases}, \tag{7}$$

where $\beta^*(d) = \frac{1}{d}\left(\frac{M}{C}\right)^2 = \beta f(q_0)$. We denote $\beta^*(d)$ as β^*.

3.2 Functional Analytic Preliminaries

We denote $\mathbb{R} = (-\infty, \infty)$, and $z = (x,q) \in Z \doteq \mathbb{R}^2$, a 2-dimensional linear vector space over reals with standard inner product denoted by $< \cdot, \cdot >$. $C^k([a,b],Z)$ is used to denote the Banach space of k-times continuously differentiable functions on $[a,b]$ taking values in Z with the sup-norm topology. In particular, $C \doteq C^0([-\sqrt{d},0],Z)$ is a Banach space of continuous functions mapping interval $[-\sqrt{d},0]$ into $\mathbb{R}$ with sup-norm

$$|\phi| = \sup_{-\sqrt{d} \le \theta \le 0} |\phi(\theta)| \quad \text{for} \quad \phi \in C. \tag{8}$$

For a continuous function of time $z(t) \in C(\mathbb{R}, Z)$, we define

$$z_t(\theta) \doteq z(t+\theta) \quad \text{for} \quad -\sqrt{d} \le \theta \le 0. \tag{9}$$

Now, it is convenient to think of the DDE (5)-(6) as an evolution equation on C. Explicitly, one can write

$$\frac{\partial z(t+\theta)}{\partial t} = \begin{cases} \partial z(t+\theta)/\partial\theta & \text{for} \quad -\sqrt{d} \le \theta < 0 \\ F(z_t, \beta) & \text{for} \quad \theta = 0 \end{cases}, \tag{10}$$

where

$$F(z_t, \beta) \doteq \begin{bmatrix} \kappa\left[\frac{1}{d} - \beta x(t)x(t-\sqrt{d})p(t-\sqrt{d})\right] \\ Mx(t) - C \end{bmatrix}. \tag{11}$$

About an equilibrium solution $z_0 = (x_0, q_0)$, the linearization is given by

$$\frac{\partial z_1(t+\theta)}{\partial t} = \begin{cases} \partial z_1(t+\theta)/\partial\theta & \text{if } -\sqrt{d} \le \theta < 0 \\ L(\beta)(z_1)_t & \text{if } \theta = 0, \end{cases} \tag{12}$$

where

$$L(\beta)(z_1)_t = \begin{bmatrix} -\kappa x_0\left[\beta^*\left(x_1(t) + x_1(t-\sqrt{d})\right) + \beta x_0 f'(q_0) q_1(t-\sqrt{d})\right] \\ Mx_1(t) \end{bmatrix},$$

and $z_1 = (x_1, q_1)^T$; subscript 1 will often be used to clarify that z_1 is a perturbation about the equilibrium z_0. For notational purposes, we will often denote the two equations (at $\theta = 0$) as

$$\frac{\partial z}{\partial t}(t) = F(z_t, \beta), \quad \text{and} \quad \frac{\partial z_1}{\partial t}(t) = L(\beta)(z_1)_t. \tag{13}$$

Here $F : U \times V \to Z$ where U and V denote open sets such that $z_0 \in U \subset C$, $\beta_0 \in V \subset \mathbb{R}$. $L(\beta) = D_z F(z_0, \beta)$ is the Frechet derivative of F taken with respect to z at (z_0, β). Associated with $L(\beta)$ is its adjoint:

$$\begin{bmatrix} -\kappa x_0 \beta^* \cdot \left[x_1(t) + x_1(t+\sqrt{d})\right] + Mq_1(t) \\ -\kappa\beta x_0^2 f'(q_0) x_1(t+\sqrt{d}) \end{bmatrix} \doteq L^*(\beta)(y_1)_t \tag{14}$$

where $y_1 = (x_1, q_1)^T$.

3.3 Eigenvalue Calculations

On taking the Laplace Transform of the linearization (12), one obtains an eigenvalue problem

$$\sigma \begin{bmatrix} X_1 \\ Q_1 \end{bmatrix} = L(\beta) \begin{bmatrix} X_1 \\ Q_1 \end{bmatrix}, \tag{15}$$

where

$$L(\beta) = \begin{bmatrix} -\kappa x_0 \beta^*(1 + e^{-\sigma\sqrt{d}}) & -\kappa\beta x_0^2 f'(q_0) e^{-\sigma\sqrt{d}} \\ M & 0 \end{bmatrix} \tag{16}$$

and $Z_1(\sigma) = (X_1, Q_1)^T(\sigma)$ is a Laplace transform of $z_1(t) = (x_1, q_1)^T(t)$. $\mathscr{L}$ is defined by the 2×2 operator matrix. In general, the operator L may have both a continuous and a discrete spectrum. In this paper, we only evaluate the discrete spectrum; details regarding continuous spectrum appear in Wang (2007).

Let $(X_1, Q_1)^T$ denote the eigenvector corresponding to an eigenvalue σ. Solving for X_1 yields

$$X_1 = \frac{-\kappa\beta \cdot x_0^2 f'(q_0) Q_1 \cdot e^{-\sigma\sqrt{d}}}{\sigma + \kappa \cdot x_0 \beta^* \cdot \left(1 + e^{-\sigma\sqrt{d}}\right)}, \tag{17}$$

provided that the denominator never vanishes, i.e., $\sigma \neq -\kappa \cdot x_0\beta^* \cdot \left(1 + e^{-\sigma\sqrt{d}}\right)$ for any d. The characteristic equation is given by:

$$1 + \frac{\kappa x_0 \left(\beta^* \sigma + M \cdot \beta x_0 f'(q_0)\right) e^{-\sigma\sqrt{d}}}{\sigma(\sigma + \kappa x_0 \beta^*)} = 0 \tag{18}$$

which is numerically solved to obtain the discrete spectrum; see Wang (2007) for details. Figure 2(a) depicts the root locus of the least stable eigenvalue pair, denoted as $\lambda(\beta)$, as it crosses the imaginary axis for increasing values of the parameter β.

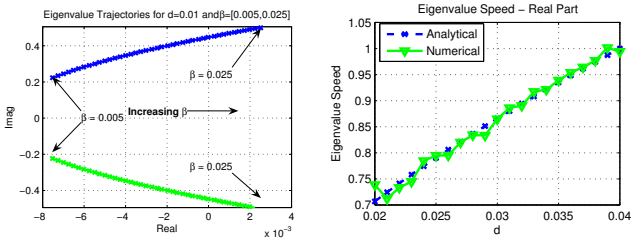

(a) (b)

Fig. 2. (a) Critical eigenvalues, and (b) Real part of eigenvalue speed at critical point

We will use the notation $\beta_0(d)$ to denote the critical value where the eigenvalue $\lambda(\beta_0) = i\omega_0$. At the critical value, the eigenvector is denoted by $Z_1(\beta_0) = (\chi_1, \phi_1)^T \doteq \zeta$. One can also repeat these considerations for the adjoint problem (equation (14)). At the critical value, $Y_1(\beta_0) = (\chi_1^*, \phi_1^*)^T \doteq \upsilon$ is used to denote the eigenvector for the adjoint problem, i.e., $L^*(\beta_0)Y_1(\beta_0) = -i\omega_0 Y_1(\beta_0)$, where L^* denotes the Laplace transform of the adjoint operator $\mathscr{L}^*$.

Spectral analysis shows that there is a single path of eigenvalue $\lambda(\beta)$ that cross the imaginary axis at the critical value $\beta = \beta_0(d)$. This suggests appearance of oscillations via a classical Hopf bifurcation analysis. To conclude a Hopf bifurcation result, one require an estimate of the eigenvalue speed at the crossover. Although, one can directly take a derivative of the characteristic equation (18), we provide this estimate in terms of operator $\mathscr{L}$ and its adjoint. The formulas will be useful in the perturbation calculations given in the following section.

Denoting

$$A(\beta) = \begin{bmatrix} 0 & -\kappa x_0^2 f'(q_0) e^{-\lambda(\beta)\sqrt{d}} \\ 0 & 0 \end{bmatrix}, \tag{19}$$

$$B(\beta) = \begin{bmatrix} \kappa\beta^*\sqrt{d}x_0 e^{-\lambda(\beta)\sqrt{d}} & \kappa\beta\sqrt{d}f'(q_0)x_0^2 e^{-\lambda(\beta)\sqrt{d}} \\ 0 & 0 \end{bmatrix}, \tag{20}$$

we obtain the following formula

$$\frac{d\lambda}{d\beta}(\beta_0) = \frac{< A(\beta_0)\zeta, \upsilon >}{< \zeta, \upsilon > - < B(\beta_0)\zeta, \upsilon >} \tag{21}$$

The details appear in Wang (2007), where we further simplify the expression to obtain a crisp formula. Here we provide a numerical comparison of the eigenvalue speed using (21) and numerical experiments; see Figure 2(b). Note, at $\beta = \beta_0$, one substitutes $\lambda(\beta_0) = i\omega_0$ in (19)-(20) and we will use the notation $A(\beta_0, \omega_0)$ and $B(\beta_0, \omega_0)$ to make this dependence explicit.

4. NONLINEAR ANALYSIS

The purpose of this section is to describe a perturbation method to obtain the oscillation solutions past-bifurcation. Using these methods, one can easily study the effect of parameters such as β and d on the post-bifurcation behavior. Details on some of these studies appear in Wang (2007).

4.1 Functional Analytic Preliminaries

We are interested in periodic solutions of (5)-(6). For study of such solutions, it is useful to introduce a substitution $s = \omega t$ to rescale the unknown period $2\pi/\omega$ to 2π. Explicitly, one obtains

$$\begin{aligned} \omega\frac{\partial z(s)}{\partial s} &= \begin{bmatrix} \kappa\left[\frac{1}{d} - \beta x(s)x(s-\omega\sqrt{d})p(s-\omega\sqrt{d})\right] \\ Mx(s) - C \end{bmatrix} \\ &\doteq \tilde{F}(z_s, \omega, \beta) \end{aligned} \tag{22}$$

where $\tilde{F}(z_s, \omega, \beta) = F(z_s(\omega\cdot), \beta)$. In the re-scaled coordinate, the linearization is given by

$$\begin{aligned} &\omega_0\frac{\partial z_1}{\partial s}(s) \\ &= \begin{bmatrix} -\kappa x_0\left[\beta^*\left(x_1(s) + x_1(s-\omega_0\sqrt{d})\right) + \beta_0 x_0 f'(q_0) q_1(s-\omega_0\sqrt{d})\right] \\ Mx_1(s) \end{bmatrix} \\ &\doteq \tilde{L}(\beta_0, \omega_0)(z_1)_s, \end{aligned} \tag{23}$$

where $\tilde{L}(\beta_0, \omega_0)(z_1)_s = D_z F(z_0, \beta_0) z_s(\omega_0\cdot) = L(\beta_0)(z_1)_s$. Note that the unknown frequency ω now appears in the right hand side of equations too.

For analysis of periodic solutions, $C^k_{2\pi}(\mathbb{R}, Z)$ is used to denote the Banach space of k-times continuously differentiable periodic functions with period 2π. Functional analytically, one is interested in solutions of the nonlinear operator equation

$$\tilde{G}(z, \omega, \beta)(s) \equiv \omega\frac{\partial z}{\partial s}(s) - \tilde{F}(z_s, \omega, \beta) = 0, \tag{24}$$

where $\tilde{G} : \tilde{U} \times \tilde{V} \to C^0_{2\pi}(\mathbb{R}, Z)$, and $z_0 \in \tilde{U} \subset C^1_{2\pi}(\mathbb{R}, Z)$, $(\omega_0, \beta_0) \in \tilde{V} \subset \mathbb{R}^2$. The linearization of the nonlinear operator equation is given by

$$D_z\tilde{G}(z_0, \omega_0, \beta_0) z_1(s) = \omega_0\frac{\partial z_1}{\partial s} - \tilde{L}(\beta_0, \omega_0)(z_1)_s, \tag{25}$$

where $D_z\tilde{G}(z_0, \omega_0, \beta_0) : C^1_{2\pi}(\mathbb{R}, Z) \to C^0_{2\pi}(\mathbb{R}, Z)$.

We will follow a perturbation method based on Lyapunov-Schmidt reduction to investigate zeros of (24). The crucial property here is that there is a simple eigenvalue $i\omega_0$ such that $L(\beta)(z_1)_t = i\omega_0 z_1(t)$, where $z_1(t) = \zeta e^{i\omega_0 t}$ for some function $\zeta = (\chi_1, \varphi_1) \in Z$. At this point, we also recall the notation for the eigenvalue problem for the adjoint: $L^*(\beta)(y_1)_t = -i\omega_0 y_1(t)$, where $y_1(t) = \upsilon e^{i\omega_0 t}$ for some function $\upsilon = (\chi_1^*, \varphi_1^*) \in Z$. After re-scaling, the explicit equations for adjoint L^* are:

$$\tilde{L}^*(\beta_0, \omega_0)(y_1)_s \doteq \begin{bmatrix} -\kappa\beta^* x_0\left[x_1(s) + x_1(s+\omega_0\sqrt{d})\right] + Mq_1(s) \\ -\kappa\beta_0 x_0^2 f'(q_0) x_1(s+\omega_0\sqrt{d}) \end{bmatrix} \tag{26}$$

In carrying out the Lyapunov-Schmidt reduction, one needs a Fredholm alternative condition for establishing existence of 2π-periodic solution of linear equation

$$\omega_0\frac{\partial z_1}{\partial s}(s) - \tilde{L}(z_1)_s = h(s) \tag{27}$$

where ω_0 appears due to the scaling of time; the explicit form of $\tilde{L}$ in our case is given in (23). The existence of 2π-periodic solution for the general boundary value problem (27) is related to the 2π-periodic solution of the adjoint problem, formally written as:

$$\omega_0\frac{\partial y_1}{\partial s}(s) + \tilde{L}^*(y_1)_s = 0. \tag{28}$$

Theorem 1. (Corollary 4.1 in Hale (1993)). The sufficient and necessary condition that there exist 2π-periodic solutions of (27) is

$$\int_0^{2\pi} < h(s), y_1(s) > \mathrm{d}s = 0 \tag{29}$$

for all 2π-periodic solutions y_1 of the formal adjoint problem (28).

In order to aid calculations in bifurcation study, we also define notation for two linear operators:

$$\tilde{A}(\beta_0, \omega_0)(z_1)_s \doteq \begin{bmatrix} -\kappa x_0^2 f'(q_0) q_1(s-\omega_0\sqrt{d}) \\ 0 \end{bmatrix} \tag{30}$$

$$\tilde{B}(\beta_0, \omega_0)(z_1)_s \doteq \begin{bmatrix} \kappa\sqrt{d}x_0\left[\beta^* x_1(s-\omega_0\sqrt{d}) + \beta_0 x_0 f'(q_0) q_1(s-\omega_0\sqrt{d})\right] \\ 0 \end{bmatrix}, \tag{31}$$

where $z_1 = (x_1, q_1)^T$. Note operators A and B first defined in (19)-(20) are in fact the Laplace transforms of these operators.

4.2 Perturbation Method

In this section, we present a Lyapunov-Schmidt based perturbation method to determine the nature of the bifurcation and

obtain asymptotic formulas for the periodic orbit near the bifurcation point. To do so, we introduce a small parameter ε and consider the perturbation expansion:

$$z(s) = z_0 + \varepsilon z_1(s) + \varepsilon^2 z_2(s) + \varepsilon^3 z_3(s) + \ldots, \quad (32)$$
$$\beta = \beta_0 + \varepsilon\beta_1 + \varepsilon^2\beta_2 + \varepsilon^3\beta_3 + \ldots, \quad (33)$$
$$\omega = \omega_0 + \varepsilon\omega_1 + \varepsilon^2\omega_2 + \varepsilon^3\omega_3 \ldots, \quad (34)$$

where (ω_0, β_0) are the frequency and the bifurcation parameter value at the critical point, $z_0 = (x_0, q_0)^T$ is the equilibrium value for the user and queue, and $z_i(s) = (x_i(s), q_i(s))^T$. The equilibrium solution is consistent with (7). On substituting the series in equation (22) and collecting terms, the $O(\varepsilon)$ yields the linearization

$$\omega_0 \frac{\partial z_1(s)}{\partial s} = \tilde{L}(\beta_0, \omega_0) z_1(s) \quad (35)$$

where $\tilde{L}(\beta_0, \omega_0)$ is defined in (23). Its solution is given in terms of the eigenfunction:

$$z_1(s) = \begin{cases} \chi_1 e^{is} + c.c. \\ \varphi_1 e^{i(s)} + c.c. \end{cases} \quad (36)$$

Here we recall that $(\chi_1, \varphi_1)^T \doteq \zeta$ are the eigenfunctions for $\tilde{L}(\beta_0, \omega_0)$. At this point, it is also useful to point out the solution to the adjoint problem (28), which is given by

$$y_1(s) = \begin{cases} \chi_1^* e^{is} + c.c. \\ \varphi_1^* e^{is} + c.c. \end{cases}, \quad (37)$$

where $(\chi_1^*, \varphi_1^*)^T \doteq \upsilon$ are the eigenfunction for the adjoint $\tilde{L}^*(\beta_0, \omega_0)$.

At $O(\varepsilon^2)$

$$\omega_0 \frac{\partial z_2(s)}{\partial s} = \tilde{L}(\beta_0, \omega_0) z_2(s) + h(s) \quad (38)$$

where

$$h(s) = -\omega_1 \frac{\partial z_1(s)}{\partial s} + \beta_1 \tilde{A}(\beta_0, \omega_0) z_1(s) + \omega_1 \tilde{B}(\beta_0, \omega_0) z_1'(s) + N_2(s), \quad (39)$$

where $\tilde{L}(\beta_0, \omega_0)$, $\tilde{A}(\beta_0, \omega_0)$, and $\tilde{B}(\beta_0, \omega_0)$ are defined in (23), (30), and (31), respectively and

$$N_2(s) = \begin{bmatrix} -\kappa\beta^* x_1(s) x_1(r) - \kappa\beta_0 x_0 f'(q_0) q_1(r) (x_1(s) + x_1(r)) \\ 0 \end{bmatrix}, \quad (40)$$

where $r \doteq s - \omega_0\sqrt{d}$ is used as a notational aid, $z_1'(r)$ denote the derivative of $z_1(\cdot)$, taken with respect to its arguments. By applying the Fredholm alternative (29), for the solution to exist

$$\int_0^{2\pi} < h(s), y_1(s) > \mathrm{d}s = 0 \quad (41)$$

Substituting (37) and (39) into (41), one obtain

$$\int_0^{2\pi} -i\omega_1 < z_1(s), y_1(s) > + \beta_1 < \tilde{A}(\beta_0, \omega_0) z_1(s), y_1(s) > + i\omega_1 < \tilde{B}(\beta_0, \omega_0) z_1(s), y_1(s) > + < N_2(s), y_1(s) > \mathrm{d}s = 0, \quad (42)$$

where $\tilde{A}(\beta_0, \omega_0)$ and $\tilde{B}(\beta_0, \omega_0)$ are defined in (30)-(31). Now $\int_0^{2\pi} < N_2(s), y_1(s) > \mathrm{d}s = 0$, because $N_2(s)$ has no harmonic component (a term proportional to e^{is} or e^{-is}). Substituting (36) and (37) into (42) results in the following

$$\tilde{A}(\beta_0, \omega_0)\left(\zeta e^{is} + c.c.\right) = A(\beta_0, \omega_0)\zeta e^{is} + c.c., \quad (43)$$

$$\tilde{B}(\beta_0, \omega_0) i \left(\zeta e^{is} + c.c.\right) = iB(\beta_0, \omega_0)\zeta e^{is} + c.c. \quad (44)$$

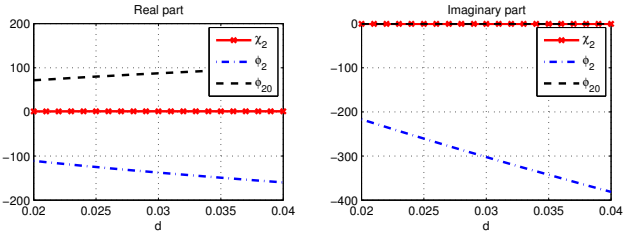

Fig. 3. Results of $z_2(s)$:(a)Real part (b)Imaginary part

Thus (42) simplifies to

$$-i\omega_1 < \zeta, \upsilon > + \beta_1 < A(\beta_0, \omega_0)\zeta, \upsilon > + i\omega_1 < B(\beta_0, \omega_0)\zeta, \upsilon >= 0. \quad (45)$$

Using formula (21), this gives

$$\frac{\mathrm{d}\lambda}{\mathrm{d}\beta}(\beta_0)\beta_1 - i\omega_1 = 0. \quad (46)$$

Since the real part of the speed is non-zero, $\beta_1 = \omega_1 = 0$. As a result of this, the $O(\varepsilon^2)$ term becomes

$$\omega_0 \frac{\partial z_2(s)}{\partial s} = \tilde{L}(\beta_0, \omega_0) z_2(s) + N_2(s) \quad (47)$$

whose solution is given by

$$z_2(s) = \begin{cases} \chi_2 e^{i2s} + c.c. \\ \varphi_2 e^{i2s} + \varphi_{20} + c.c. \end{cases}, \quad (48)$$

where χ_2, φ_2 and φ_{20} are shown in Figure 3(a)-(b).

At $O(\varepsilon^3)$, we need only apply the Fredholm alternative to deduce β_2 and ω_2, so we express the equation

$$\omega_0 \frac{\partial z_3(s)}{\partial s} = \tilde{L}(\beta_0, \omega_0) z_3(s) + h(s) \quad (49)$$

where

$$h(s) = -\omega_2 \frac{\partial z_1(s)}{\partial s} + \beta_2 \tilde{A}(\beta_0, \omega_0) z_1(s) + \omega_2 \tilde{B}(\beta_0, \omega_0) z_1'(s) + N_3(s) \quad (50)$$

where $\tilde{L}(\beta_0, \omega_0)$, $\tilde{A}(\beta_0, \omega_0)$, and $\tilde{B}(\beta_0, \omega_0)$ are defined in (23),(30) and (31),respectively. $N_3(s)$ is given by

$$N_3(s) = \begin{bmatrix} N_{3,x}(s) \\ 0 \end{bmatrix}, \quad (51)$$

where

$$\begin{aligned} N_{3,x}(s) = &-\kappa\beta^*[x_1(s)x_2(r) + x_1(r)x_2(s)] \\ &-\kappa\beta_0 f'(q_0) x_1(s) x_1(r) q_1(r) \\ &-\kappa\beta_0 x_0 f'(q_0) q_2(r)[x_1(s) + x_1(r)] \\ &-\kappa\beta_0 x_0 f'(q_0) q_1(r)[x_2(s) + x_2(r)], \end{aligned} \quad (52)$$

where $r = s - \omega_0\sqrt{d}$ is again used as a notational aid. By the Fredholm alternative, for a solution to (49) to exist, the following condition must be satisfied

$$\int_0^{2\pi} < h(s), y_1(s) > \mathrm{d}s = 0. \quad (53)$$

Substituting $h(s)$ into (53), we have

$$\int_0^{2\pi} -i\omega_2 < z_1(s), y_1(s) > + \beta_2 < \tilde{A}(\beta_0, \omega_0) z_1(s), y_1(s) > + i\omega_2 < \tilde{B}(\beta_0, \omega_0) z_1(s), y_1(s) > + < N_3, y_1(s) > \mathrm{d}s = 0.$$

Now, $\int_0^{2\pi} < N_3, \upsilon > \mathrm{d}s \neq 0$ because it contains harmonic components. We denote $\tilde{N}_3$ as the harmonic components of N_3

$$\tilde{N}_3 = \begin{bmatrix} \tilde{N}_{3,x} \\ 0 \end{bmatrix}, \tag{54}$$

where

$$\begin{aligned}\tilde{N}_{3,x} = &-\kappa\beta^*\bar{\chi}_1\chi_2\left(e^{-i2\omega_0\sqrt{d}} + e^{i\omega_0\sqrt{d}}\right)\\ &-\kappa\beta_0 f'(q_0)\left[\chi_1^2\bar{\varphi}_1 + \chi_1\bar{\chi}_1\varphi_1(1+e^{-i2\omega_0\sqrt{d}})\right]\\ &-\kappa\beta_0 x_0 f'(q_0)\bar{\chi}_1\varphi_2(e^{-i2\omega_0\sqrt{d}} + e^{-i\omega_0\sqrt{d}})\\ &-\kappa\beta_0 x_0 f'(q_0)\chi_1(\varphi_{20}+\bar{\varphi}_{20})(1+e^{-i\omega_0\sqrt{d}})\\ &-\kappa\beta_0 x_0 f'(q_0)\chi_2\bar{\varphi}_1(e^{i\omega_0\sqrt{d}} + e^{-i\omega_0\sqrt{d}}).\end{aligned}$$

On repeating the steps (43)-(45), one obtain for this case

$$\begin{aligned}&-i\omega_2 < \zeta, \upsilon > +\beta_2 < A(\beta_0,\omega_0)\zeta, \upsilon >\\ &+i\omega_2 < B(\beta_0,\omega_0)\zeta, \upsilon > + < \tilde{N}_3, \upsilon >= 0.\end{aligned} \tag{55}$$

where $\zeta = (\chi_1, \varphi_1)^T$ and $\upsilon = (\chi_1^*, \varphi_1^*)^T$. Solving the real and complex terms of (55) leads to ω_2 and β_2. The results are shown in Figure 4(a), which shows that the bifurcation is supercritical (β_2 is positive). For a particular $d = 0.022$, the resulting stable branch of the oscillations is presented in Figure 4(b).

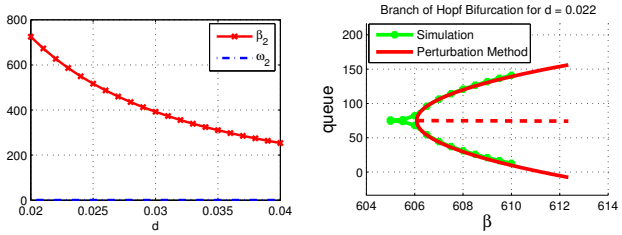

(a) (b)

Fig. 4. (a)Results of β_2 and Ω_2 and (b) the resulting stable branch of oscillations.

5. CONCLUSION

In this paper, we studied the dynamical model (1)- (2). Using numerical simulations, we found two states: equilibrium and limit-cycle oscillations. The equilibrium value was found analytically in (7), which matched the numerical results obtained with RED AQM. Using bifurcation analysis, we showed oscillations arise as a result of a supercritical Hopf bifurcation. A perturbation method was used to obtain the branch of oscillation solutions consistent with the solutions observed numerically (see Figure 4).

6. APPENDIX

$$\zeta = \begin{pmatrix}\chi_1\\ \varphi_1\end{pmatrix} = \begin{pmatrix}1\\ \frac{M}{i\omega_0}\chi_1\end{pmatrix} \quad \upsilon = \begin{pmatrix}\chi_1^*\\ \varphi_1^*\end{pmatrix} = \begin{pmatrix}1\\ \frac{\kappa\beta_0 x_0^2 f'(q_0)e^{i\omega_0\sqrt{d}}}{i\omega_0}\chi_1^*\end{pmatrix} \tag{56}$$

$$\chi_2 = \frac{-\kappa\chi_1^2 e^{-i\omega_0\sqrt{d}}\left[\beta^* + \beta_0 x_0 f'(q_0)\frac{M}{i\omega_0}(1+e^{-i\omega_0\sqrt{d}})\right]}{i2\omega_0 + \kappa x_0\left[\beta^*(1+e^{-i2\omega_0\sqrt{d}}) + \beta_0 x_0 f'(q_0)\frac{M}{i2\omega_0}e^{-i2\omega_0\sqrt{d}}\right]} \tag{57}$$

$$\varphi_2 = \frac{M}{i2\omega_0}\chi_2 \tag{58}$$

$$\varphi_{20} = -\frac{\beta^*\chi_1\bar{\chi}_1 e^{i\omega_0\sqrt{d}}}{\beta_0 x_0^2 f'(q_0)} - \frac{\bar{\varphi}_1\chi_1(1+e^{i\omega_0\sqrt{d}})}{x_0} \tag{59}$$

REFERENCES

T. Alpcan and T. Başar. A utility-based congestion control scheme for Internet-style networks with delay. **IEEE Transactions on Networking**, 13(6):1261–1274, December 2005.

Joel Ariaratnam. **Collective Dynamics of the WinFree Model of Coupled NonLinear Oscillators**. PhD thesis, Cornell University, May 2002.

V. Firoiu and M. Borden. A study of active queue management for congestion control. In **Proc. IEEE Infocom**, Tel Aviv, Israel, March 2000.

J.K. Hale. **Introduction to Functional Differential Equations**. Number 99 in Applied Mathematical Sciences. Springer, 1993.

H. Han, C.V. Hollot, D. Towsley, and Y. Chait. Synchronization of tcp flows in networks with small droptail buffers. In **Proc. of the 44th IEEE Conference on Decision and Control**, pages 6762–67, Seville, Spain, December 2005.

C. V. Hollot, V. Misra, D. Towsley, and W.B. Gong. Analysis and design of controllers for AQM routers supporting TCP flows. **IEEE Transactions on Automatic Control**, pages 945–959, June 2002.

Erman Korkut. Limit cycling in tcp networks. Master's thesis, Univeristy of Massachusetts Amherst, September 2006.

R. J. La, Priya Ranjan, and Eyad H. Abed. Bifurcation TCP and UDP traffic under RED. In **MED**, 2002.

C. Li, G. Chen, X. Liao, and J. Yu. Hopf bifurcation in an internet congestion control model. **Chaos, Solitons, and Fractals**, 19:853–862, 2004.

Gaurav Raina. Local bifurcation analysis of some dual congestion control algorithms. **IEEE Transactions on Automatic Control**, 50:1135–1144, 2005.

Priya Ranjan and Eyad H. Abed. Bifurcation analysis of TCP-RED dynamics. In **Proc. of the American Control Conference**, Anchorage, AK, May 2002.

S. Shakkottai, R. Srikant, and S. Meyn. Bounds on the throughput of congestion controllers in the presence of feedback delay. In **Proceedings of the IEEE Conference on Decision and Control**, Florida, USA.

S. Shakkottai, R. Srikant, and S. P. Meyn. Bounds on the throughput of congestion controllers in the presence of feedback delay. **IEEE/ACM Transactions on Networking**, 11 (6):972–981, December 2003.

R. Srikant. **The Mathematics of Internet Congestion Control**. Systems & Control: Foundations & Applications. Birkhauser, Boston, MA, 2004.

A. Veres and M. Boda. The chaotic nature of TCP congestion control. In **Proc. IEEE Infocom**, volume 3, pages 1715–1723, March 2000.

Pang Paul Wang. Synchronization of delay-differential equations in communication networks. Master's thesis, University of Illinois at Urbana-Champaign, August 2007.